Class. Quantum Grav. **25** (2008) 114030 (8pp) doi:10.1088/0264-9381/25/11/114030

dc readout experiment at the Caltech 40m prototype interferometer

R L Ward[1], R Adhikari[1], B Abbott[1], R Abbott[1], D Barron[4], R Bork[1], T Fricke[1], V Frolov[2], J Heefner[1], A Ivanov[1], O Miyakawa[1], K McKenzie[3], B Slagmolen[3], M Smith[1], R Taylor[1], S Vass[1], S Waldman[1] and A Weinstein[1]

[1] LIGO Caltech 18-34, Pasadena, CA 91125, USA
[2] LIGO Livingston Observatory, Livingston, LA 70754, USA
[3] Australian National University, Canberra, ACT 0200, Australia
[4] University of Illinois at Urbana-Champaign, Urbana, IL 61801, USA

E-mail: rward@ligo.caltech.edu

Received 31 October 2007, in final form 17 December 2007
Published 15 May 2008
Online at stacks.iop.org/CQG/25/114030

Abstract

The Laser Interferometer Gravitational Wave Observatory (LIGO) operates a 40m prototype interferometer on the Caltech campus. The primary mission of the prototype is to serve as an experimental testbed for upgrades to the LIGO interferometers and for gaining experience with advanced interferometric techniques, including detuned resonant sideband extraction (i.e. signal recycling) and dc readout (optical homodyne detection). The former technique will be employed in Advanced LIGO, and the latter in both Enhanced and Advanced LIGO. Using dc readout for gravitational wave signal extraction has several technical advantages, including reduced laser and oscillator noise couplings as well as reduced shot noise, when compared to the traditional rf readout technique (optical heterodyne detection) currently in use in large-scale ground-based interferometric gravitational wave detectors. The Caltech 40m laboratory is currently prototyping a dc readout system for a fully suspended interferometric gravitational wave detector. The system includes an optical filter cavity at the interferometer's output port, and the associated controls and optics to ensure that the filter cavity is optimally coupled to the interferometer. We present the results of measurements to characterize noise couplings in rf and dc readout using this system.

PACS number: 04.80.Nn

(Some figures in this article are in colour only in the electronic version)

1. Introduction

There is now underway a worldwide effort to detect gravitational waves, ripples in spacetime which carry information about astrophysical events. The currently running kilometer-scale interferometric gravitational wave detectors (LIGO [1], VIRGO [2], GEO [3] and TAMA [4]) have demonstrated an unprecedented sensitivity to strain (the squeezing and stretching of space which is the local effect of a gravitational wave), reaching $\approx 10^{-22}$ at 100 Hz in the case of LIGO. Achieving such a sensitivity has been the result of significant effort to reduce, mitigate, and avoid, the multitudinous sources of noise which can mask the effect of gravitational waves. Future detectors, including Enhanced LIGO [5] (online in 2009) and Advanced LIGO [6] (online in 2014) plan to use a technique known as *dc readout* which is expected to provide technical advantages in avoiding several sources of noise.

We have undertaken an experiment to characterize a dc readout scheme using the Caltech 40m prototype interferometric gravitational wave detector, which is used to test systems integration and advanced interferometric techniques for future LIGO detectors. It is a fully instrumented prototype, with sensing and control systems (including optical and electronic hardware) as similar as possible to those used in LIGO. It is equipped with a LIGO-style pre-stabilized laser (PSL) [7], the core optics of the interferometer are suspended from single pendulums, and most of the many control loops ($\approx$65) are implemented in a highly flexible and integrated digital system [8]. This digital control system allows us to operate the interferometer in multiple configurations (i.e., rf and dc readout) with a minimal switching overhead, and provides the ability to measure multiple transfer functions (e.g. noise couplings) simultaneously. We have measured noise couplings for an interferometer topology similar to that of LIGO and Enhanced LIGO: a Michelson interferometer, operated on a dark fringe, whose end mirrors have been replaced by Fabry–Perot cavities, and which has a partially reflecting mirror between the laser and the input port (a power recycling mirror). See figure 1 for a diagram of such a power-recycled Fabry–Perot Michelson interferometer.

2. Gravitational wave signal readout

2.1. rf readout

A common technique in precision laser interferometry involves frontal phase modulation of laser light prior to its injection into the interferometer, followed by coherent demodulation at various ports (including the output port) of the interferometer. The frontal modulation of the input laser light produces modulation sidebands (typically at radio frequencies) around the main carrier frequency of the laser light. The carrier and modulation sidebands experience different resonant conditions in the interferometer. With the proper choice of cavity lengths and modulation frequencies, optically heterodyning these light fields permits the extraction of non-degenerate signals containing information about the state of an interferometer, in particular the various length degrees of freedom [9]. In this paper, the term *rf readout* will refer to the use of this technique for sensing length changes of the differential arm (DARM) degree of freedom, which is the degree of freedom sensitive to gravitational wave strain. For audio frequency gravitational waves incident on the interferometer, the gravitational wave signal takes the form of audio sidebands around the laser carrier light at the output port. At the photodetector, these sidebands then beat against the rf modulation sidebands, which serve as a local oscillator. The gravitational wave signal sidebands are then present in the photocurrent as audio frequency sidebands around the rf modulation frequency. This rf photocurrent is electronically mixed

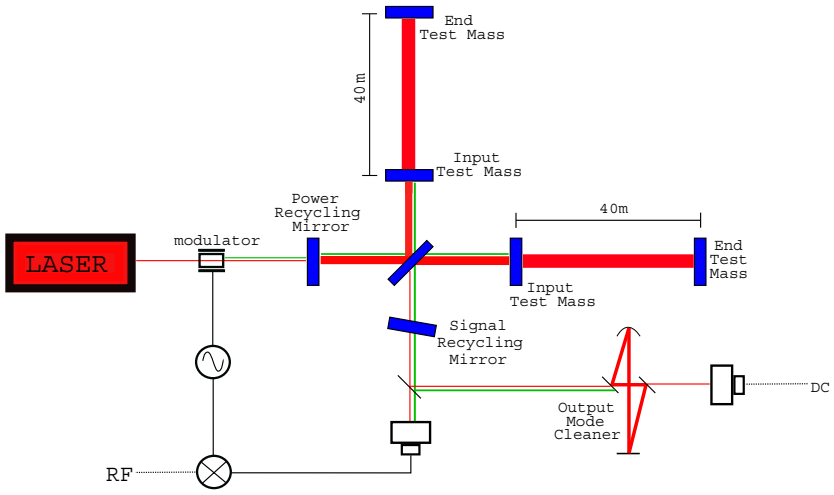

Figure 1. Schematic representation of the interferometer configuration. The 40m interferometer is currently configured as a detuned resonant sideband extraction interferometer similar to the projected configuration for Advanced LIGO, and is thus equipped with a signal recycling mirror (SRM) at the asymmetric port. For the results in this paper, we purposely misaligned the SRM in such a way that it behaves as a large loss without otherwise affecting the dynamics of the interferometer; the results thus apply to power-recycled Fabry–Perot Michelson interferometers, such as LIGO and Enhanced LIGO. In this figure, the red beam represents the laser carrier field and the green beam the rf sideband field.

down to baseband before being acquired digitally. A more detailed discussion of this control scheme can be found in [10], and an analysis of the effects of laser and rf oscillator noise in power-recycled Fabry–Perot Michelson interferometers in [11].

2.2. dc readout

A complementary technique for gravitational wave signal readout is to arrange the optics of the interferometer in such a way that the power present at the output port of the interferometer is directly proportional to gravitational wave strain. This technique is a form of optical homodyne detection known as *dc readout*, in which laser carrier light that has circulated in the interferometer serves as a local oscillator, rather than rf modulation sidebands. In the case of kilometer-scale gravitational wave detectors, dc readout can provide a significant advantage in terms of reducing susceptibility to two sources of technical noise: laser noise and rf oscillator noise. The reason for this advantage is the different behavior of the rf modulation sidebands and the laser carrier light in the interferometer: the carrier light enters the kilometer-scale arm cavities and thus undergoes a stage of passive low-pass filtering by the interferometer, while the modulation sidebands do not experience any significant filtering [12]. Any noise on the modulation sidebands (whether from the laser itself or the modulator) thus passes essentially unchanged to the detection port of the interferometer, where it can pollute the signal when the modulation sidebands are used as a local oscillator (in rf readout). Additionally, in dc readout, as both the local oscillator and the signal are coming from the same place (i.e., the arm cavities of the interferometer), they are in the same transverse spatial mode and thus have perfect spatial overlap at the photodetector. In its simplest form, dc readout involves intentionally causing a small offset in the DARM degree of freedom, which slightly spoils the destructive interference at the output port of the interferometer, allowing a small amount of light to leak

out for use as a local oscillator. For small deviations from the controlled setpoint of DARM, the power at the output port is linearly proportional to deviations from resonance, and is thus sensitive to tiny changes in the lengths of the arm cavities. An analytical comparison of susceptibility to laser noise in rf/dc readout schemes was carried out in [13].

3. dc readout experiment

3.1. Methods and equipment

dc readout removes the need for the rf sidebands used as local oscillators for rf readout. We take advantage of this fact by inserting an output mode cleaner (OMC) in the optical sensing chain at the output port of the interferometer, before the dc photodetector. This output mode cleaner (OMC) serves to reject the rf modulation sidebands and 'junk light' (light that does not share the same spatial or polarization mode as the signal mode) exiting the output port of the interferometer, both of which contribute noise but not signal. We have constructed an OMC composed of a monolithic, four-mirror bowtie shaped resonant cavity with a finesse of 210. The OMC is kept on resonance with the interferometer carrier light via PZT length actuation; the OMC length is dithered at a frequency outside of the gravitational wave band for sensing this length degree of freedom. The bandwidth of the control loop is 100 Hz. The angular degrees of freedom of the OMC (beam tilt and displacement relative to the mode of interferometer) are controlled by a pair of PZT actuated steering mirrors situated between the output port of the interferometer and the OMC; sensing of these degrees of freedom is also via dithering. Limitations on the actuators require that this dithering remain in the detection band. There is a fixed mode-matching telescope between the interferometer and the OMC, which brings the mode matching to approximately 93%. Light transmitted through the OMC is directed to a pair of photodetectors; the photodetectors are each wired in series with transimpedance resistors, and the voltage across the resistors is amplified and whitened by a low-noise circuit. All of the equipment described above is enclosed in the same vacuum envelope as the main interferometer, and mounted on optical tables atop seismic isolation stacks (see figure 2). The amplified photodetector signal is acquired digitally for use in the digital control system and measurement of transfer functions. The dc readout sensing chain receives 60% of the light exiting the output port of the interferometer; the remaining 40% is sent to a traditional rf readout sensing chain to be used for lock acquisition, signal extraction of auxiliary degrees of freedom, and dc/rf comparisons. The digital control system used for the dc readout chain (consisting primarily of OMC length and alignment controls) is of the type projected for use in Advanced LIGO. The successful integration of this system with the rest of our LIGO-style electronic infrastructure represents a significant milestone for Enhanced LIGO, which will employ a similar mixture.

3.2. Results and modeling

We model the interferometer response using a frequency-domain interferometer simulation tool [14] which includes the effects of radiation pressure, and compare the results from this model for laser frequency and intensity noise with the measured transfer functions from the interferometer in both a dc readout configuration and an rf readout configuration. The design parameters for the input test mass and power recycling mirror power transmissivities, which affect the interferometer dynamics most, are $T_{\mathrm{ITM}} = 0.005$ and $T_{\mathrm{PRM}} = 0.07$. For modeling laser noise couplings, of greatest interest are the mismatches between the two arm cavities. The round trip loss mismatch has been independently measured to be 20 ppm (from an average

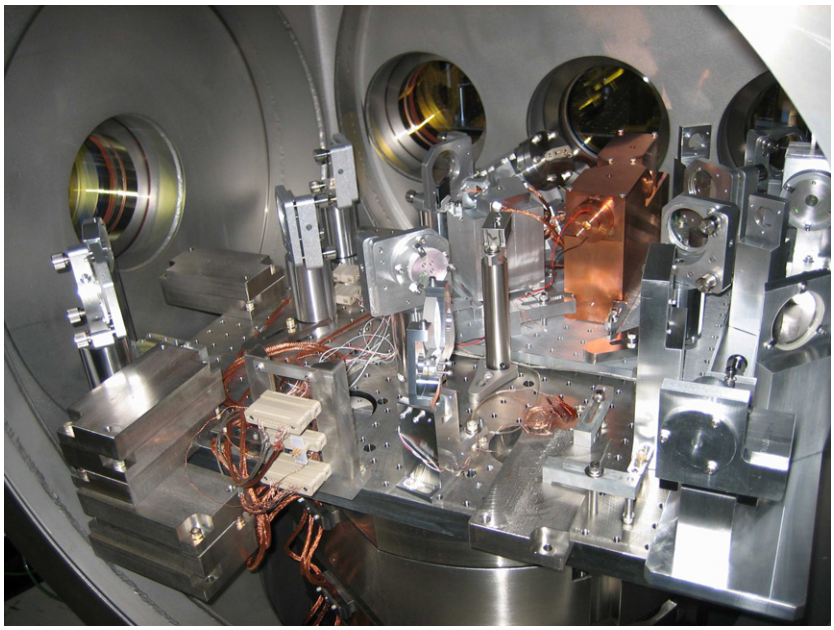

Figure 2. The dc readout sensing chain. Visible on the table are one PZT steering mirror, the mode-matching telescope, the output mode cleaner (made of copper to damp vibrational modes), the dc photodetectors and other optics.

of 160 ppm) and the ITM transmissivity mismatch been determined to be 9% by a fit to the data. The static differential arm length offset for dc readout was ≈25 pm, chosen to minimize the effect of electronics and ADC noise. We also present the results of measurements of oscillator phase and amplitude noise couplings, but we do not yet have modeling tools for these.

3.2.1. Laser frequency noise. The 40m interferometer is equipped with a common mode servo, which alters the frequency of the primary laser light in order to match the length of the common mode arm length (CARM). The coupling of laser frequency noise to the gravitational wave signal is minimized by the designed symmetries of the interferometer; however, imbalances in the two arms of the interferometer can allow laser noise to leak through from the input port to the output port. The noise coupling was measured in this case by injecting a signal at the error point of the common mode servo, inducing a frequency mismatch between the laser light and the CARM degree of freedom; the signal was then coherently demodulated in the gravitational wave channel to determine the transfer function. The measured results (figure 3(*a*)) agree with the model above ≈1 kHz, but there remains a significant unexplained discrepancy at lower frequencies. The asymptotic behavior appears well modeled, however, and implies that dc readout will provide a real advantage within the gravitational wave detection band when employed in large-scale detectors (which have much larger time constants than the 40m interferometer, and should thus asymptote at much lower frequencies).

3.2.2. Laser intensity noise. The PSL includes an intensity stabilization servo which stabilizes intensity fluctuations of the laser light prior to its injection into the interferometer.

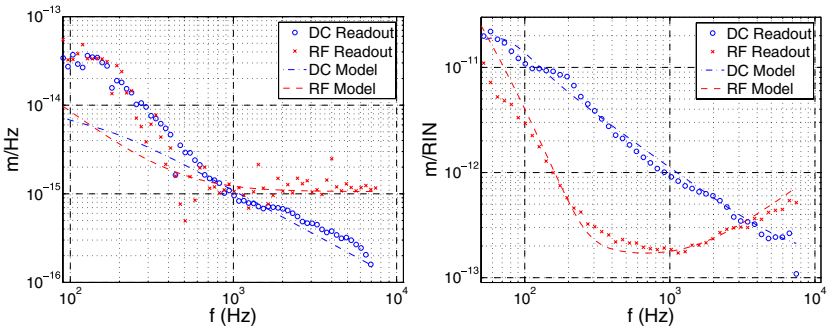

(a) Frequency noise coupling (b) Intensity noise coupling

Figure 3. Laser noise coupling for the 40m Fabry–Perot Michelson interferometer with power recycling. The dots indicate experimental data while the dashed lines indicate the results of numerical simulation.

By injecting a signal into the error point of this servo, we can introduce controlled levels of intensity fluctuations and measure the transfer function from laser intensity noise to the gravitational wave readout channel. These measurements (figure 3(b)) agree well with the modeled results; as predicted for the 40m interferometer, the coupling of intensity noise is much larger in the dc readout scheme. For kilometer-scale interferometers, this coupling will be greatly reduced by the increased light storage time of the system, while the coupling for the rf readout scheme will be largely unchanged.

3.2.3. Oscillator phase noise. A IFR2023A signal generator is used as the source signal for the rf modulation sidebands on the laser light, and the same oscillator signal is then used in demodulating the signal. This model is equipped with a external modulation port, which allows external modulation of the phase and amplitude of the oscillator signal. We use this feature to measure the transfer functions described in this section and in section 3.2.4. As the rf modulation sidebands are not filtered by the interferometer, any phase noise on the oscillator should appear in both the rf photocurrent which is the product of optical heterodyning and the electronic local oscillator with which the rf photocurrent is further heterodyned to baseband. In this final stage of mixing, oscillator phase noise should cancel and disappear from the signal; in practice, for reasons which are not wholly understood, it does not. For LIGO this was a limiting noise source above $\sim$1 kHz during 2004. It is not known whether the solution currently in use (lower noise oscillators) will be feasible for Advanced LIGO. In the dc readout scheme, the rf sidebands are not used for gravitational wave signal extraction, and thus have a much reduced opportunity to pollute the signal; potential coupling routes include (1) noise impressed onto auxiliary degrees of freedom (e.g., CARM or the Michelson degree of freedom) which can then couple to the DARM signal and (2) direct sideband leakage through the OMC (which should nominally reject them). Refer to figure 4(a) for the results of measurements showing a significant improvement for dc readout.

3.2.4. Oscillator amplitude noise. In the rf readout scheme, any amplitude noise on the oscillator used to generate the rf modulation sidebands will appear after optical heterodyning as a gain modulation. If there is a residual, static offset in the signal, then this amplitude noise can appear directly; otherwise it appears bilinearly with the DARM signal. In the dc readout scheme, the rf modulation sidebands are used for sensing and control of auxiliary degrees of freedom, and so noise on these sidebands can couple indirectly to DARM. Additionally, as

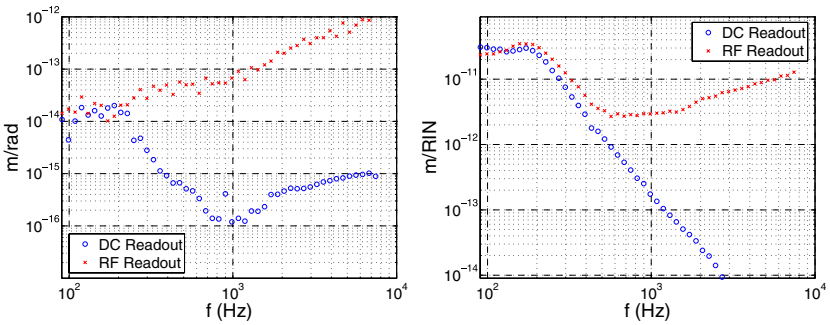

(*a*) Oscillator phase noise coupling (*b*) Oscillator amplitude noise coupling

Figure 4. Oscillator noise coupling for the 40m Fabry–Perot Michelson interferometer with power recycling. The dots indicate experimental data.

the rf modulation sidebands extract power from the carrier, any amplitude fluctuations on the sidebands correspond to amplitude fluctuations on the carrier, which can manifest as intensity noise. Direct rf sideband leakage through the OMC can also contribute. Refer to figure 4(*b*) for the results of measurements showing a significant improvement for dc readout.

3.2.5. Displacement noise. Although the Caltech 40m interferometer is not intended as a low-noise prototype, it is nonetheless interesting to compare the achieved displacement sensitivities in rf and dc readout configurations. The total displacement noise is broadly similar for both rf and dc readout, with both configurations achieving the same noise minimum of $2 \times 10^{-18} \frac{\mathrm{m}}{\sqrt{\mathrm{Hz}}}$ near 1 kHz. Above ∼1 kHz, rf readout shows a greater susceptibility to laser frequency noise, which conforms to expectations from the measured transfer functions (figure 3(*a*)). The dc readout noise spectrum has shown a small excess over that of rf readout between 100–400 Hz. The source of this noise is currently unknown, but as of this writing we have not carried out exhaustive efforts to identify it. The noise in dc readout has also been shown to be sensitive to the static alignment of the beam entering the OMC, although we have not seen evidence of input beam jitter noise when there is not a significant static misalignment.

4. Conclusions

We have carried out an experiment to characterize a dc readout scheme on a suspended-mass power-recycled Fabry–Perot Michelson interferometer, using a seismically isolated in-vacuum output mode cleaning cavity along with an in-vacuum photodetector. We have demonstrated that the laser noise couplings in rf/dc readout schemes behave as expected and that oscillator noise couplings are significantly reduced in the dc readout scheme. These results represent an important test of the dc readout system planned for Enhanced LIGO and Advanced LIGO.

Acknowledgments

LIGO was constructed by the California Institute of Technology and Massachusetts Institute of Technology with funding from the National Science Foundation and operates under cooperative agreement PHY-0107417. This paper has LIGO document number LIGO-P070125-00-Z.

References

[1] Abramovici A *et al* 1992 *Science* **256** 325–33
[2] Acernese F *et al* 2002 *Class. Quantum Grav.* **19** 1421
[3] Willke B *et al* 2002 *Class. Quantum Grav.* **19** 1377
[4] Ando M and (The TAMA Collaboration) 2002 *Class. Quantum Grav.* **19** 1409
[5] Adhikari R, Fritschel P and Waldman S 2006 *LIGO Report no LIGO-T060156-01*
[6] Fritschel P 2003 *Proc. SPIE-Int. Soc. Opt. Eng.* **4856** 282
[7] Savage R, King P and Seel S 1998 *Laser Phys.* **8** 679–85
[8] Bork R, Abbott R, Barker D and Heefner J 2001 *Proc. ICALEPCS (San José, CA, 27–30 November, 2001)* 19–23 (eConf C011127)
[9] Regehr M 1994 *LIGO Report no LIGO-P940002-00-I*
[10] Fritschel P *et al* 2001 *Appl. Opt.* **40** 4988–98
[11] Camp J *et al* 2000 *J. Opt. Soc. Am.* A **17** 120
[12] Sigg D and (The ISC Group) 1997 *LIGO Report no LIGO-T970084-00 D*
[13] Somiya K *et al* 2006 *Phys. Rev.* D **73** 122005
[14] Evans M 2007 *LIGO Report no LIGO-T070260-00*